ACIS Instrument Team

report

MIT Center for Space Research
1 Hampshire Street
Cambridge, MA 02139-4307

Tel: 617-253-7277
Fax: 617-253-8084

Date: June 4, 2002

To: ACIS Instrument Team

From: Peter G. Ford, NE80-6071 <pgf@space.mit.edu>

Re: ACIS CC-Mode Bias Algorithm

Cc: Chandra Science Operations Team

All one-dimensional bias maps computed for ACIS front-illuminated CCDs in continuous-clocking mode show systematic errors of tens of ADU in some columns. These anomalies are caused by the presence of clouds of background charge that typically cover several percent of each front-illuminated CCD. Their effect on bias maps has been confirmed by CC raw-mode tests performed in the fall of 2001. Happily, a simple change in bias parameters can substantially reduce the anomalies in future bias maps. The remainder of this report discusses the evidence from continuously-clocked science runs, the analysis of the raw-mode tests, and the implications of a change to the continuous-clocking bias parameters.

Introduction

Since the end of the On-Orbit Checkout phase on 10/11/1999, ACIS has performed 64 science runs in continuous-clocking (CC) mode, generating 357 bias maps, all of which were successfully downlinked. Even a cursory inspection of the maps from front-illuminated (FI) CCDs shows them to contain obvious artifacts, *e.g.*, Figure 1, in which the maps from CCD_S2 of OBSID 85 and CCD_I3 of OBSID 668 are both seen to contain peaks > 20 ADU above the values of their mean quadrant overclocks, at column locations that have never been identified as defective in any other CC or timed-exposure (TE) run.

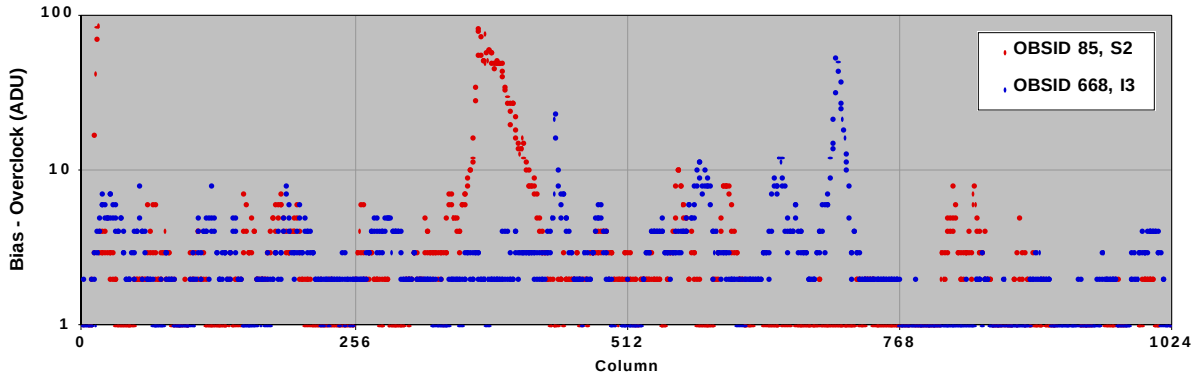

Figure 1: A pair of continuous-clocking-mode bias maps computed on orbit. The anomalously high values show up in different columns from run to run.

The situation for all 64 runs is summarized in Table 1, which shows the number of runs using each CCD, the mean value over all columns of Δ, the difference between column bias and overclock, and the average over all runs

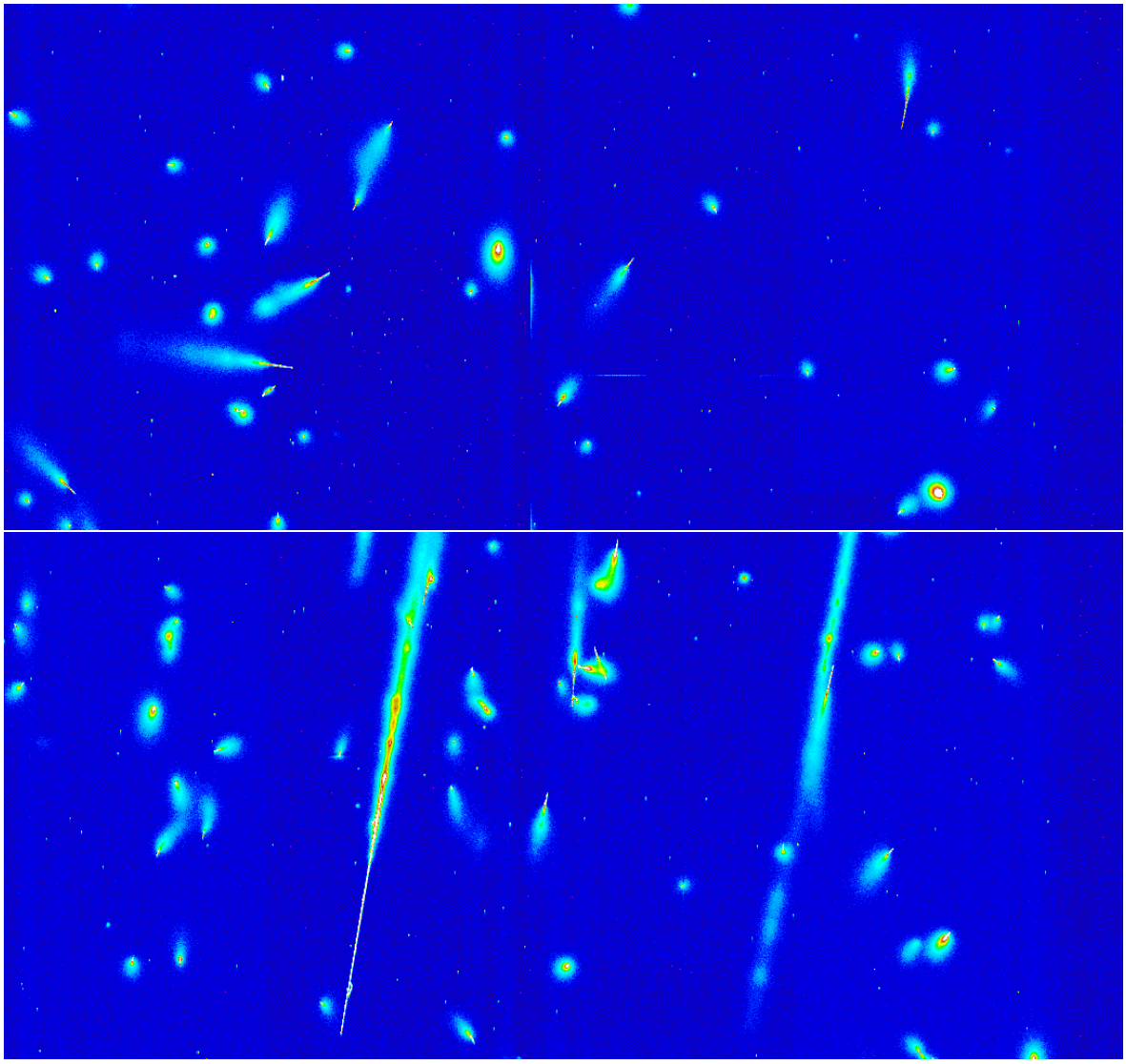

Figure 2: Raw frames 1292 and 1364 of OBSID 61543, illustrating the presence of charge tracks, some nearly parallel to the column direction (vertical).

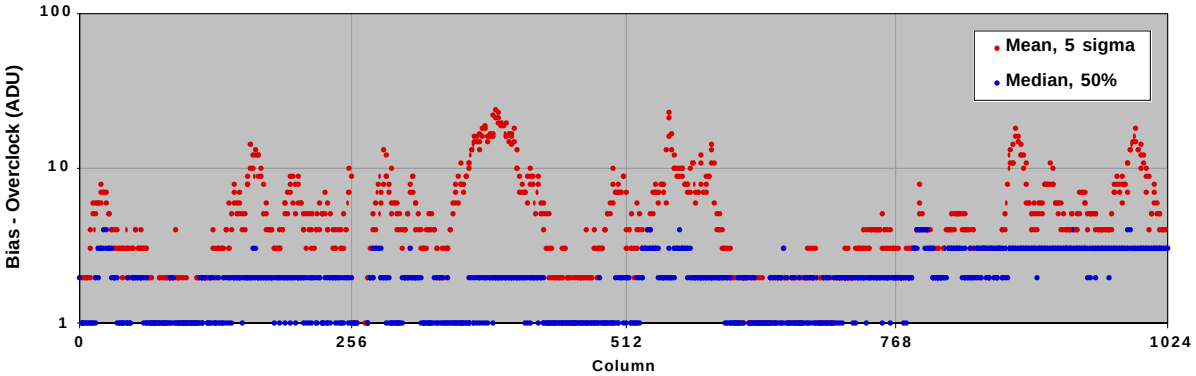

Figure 3: Bias maps constructed from the frames of Figure 2 using the *Mean* algorithm with 5 **σ** rejection (red) and the *Median* algorithm with 50% quartile (blue).

of the minimum, maximum and standard-deviation of Δ. In each case, the column to the right of these values contains its standard deviation over the runs.

All CC runs thus far have used the same on-board algorithm to compute their bias maps. It is termed Mean with *n*-σ rejection and works as follows:[1]

1. After ignoring the first 100 frames, two consecutive frames (2×512 rows) are clocked from the CCD.
2. Each column is processed independently, as follows:
3. The mean and standard-deviation of the 1024 pixels are computed.
4. Pixels that differ from the mean by more than *n* times the standard-deviation are ignored; thus far, *n* has always been 5.
5. The mean of the remaining pixels is taken as the bias value for that column.

Table 1: Distribution of bias values from all on-orbit Cc3x3 runs

CCD	*n*[a]	Δ_{mean}[b]		Δ_{min}		Δ_{max}		σ_{Δ}	
		ADU	±[c]	ADU	±[c]	ADU	±[c]	ADU	±[c]
I0	14	0.6	1.4	0.0	0.4	6.4	16.5	0.7	1.8
I1	2	3.6	0.9	0.0	0.0	43.5	11.5	4.4	2.3
I2	33	3.9	0.6	-0.7	0.6	37.1	43.9	3.4	1.5
I3	33	3.2	0.6	0.2	0.7	46.9	104.8	3.3	3.9
S0	18	3.9	1.2	0.7	0.5	30.1	24.7	3.0	1.8
S1	54	1.1[d]	0.3	0.2	0.4	4.6	2.5	0.5	0.1
S2	59	2.9	0.8	0.3	0.4	36.8	40.3	3.0	1.9
S3	62	2.2[e]	0.5	0.7	0.5	10.4	24.1	1.0	1.0
S4	57	5.3	0.7	1.9	0.3	32.5	28.9	3.0	1.8
S5	25	3.9	1.4	0.8	0.6	40.2	78.8	4.3	7.0

a. Number of CC runs using this CCD.
b. After subtracting the mean overclock value.
c. Standard deviation over *n* runs of the value in the corresponding ADU column.
d. Ignoring the first 96 pixels clocked from each node and from 8 additional bad columns.
e. Ignoring the first 96 pixels clocked from each node.

To include the back-illuminated (BI) CCDs in the analysis leading to Table 1, the first 96 pixels clocked from each output node were ignored, since the average bias value is known to change rapidly over this region. In addition, a number of columns of CCD_S1 are known to be defective and were ignored.

Analysis

Recognizing that the anomalies in the FI bias maps are caused by background events in the CCDs, a series of three tests was run in Aug-Sep 2001 with the purpose of characterizing the pattern of background charge and to devise ways of minimizing the effect that charge on bias maps.

The first test (OBSID 61543) observed 91 frames from CCD_S0, the second (OBSID 61519) took 89 frames from CCD_S2, and the third (OBSID 61507) took 85 frames from CCD_I3. Each frame comprises 512 rows of 1024 pixels, but, because of limited buffer space, only the first two or three frames were contiguous the remainder were sampled at ca. 90 second intervals. A

Table 2: Distribution of bias values from CcRaw runs, processed by various algorithms

OBSID, CCD, date	n_f[a]	Algorithm	*parm*[b]	Δ_{mean}[c]		Δ_{min}		Δ_{max}		σ_Δ	
				ADU	±[d]	ADU	±[d]	ADU	±[d]	ADU	±[d]
61543 CCD_S0 7/17/01	91	Mean	1σ	2.1	1.4	-0.4	0.5	14.0	10.9	1.5	0.4
			2σ	2.5	1.4	-0.3	0.6	19.2	13.8	2.0	0.7
			3σ	2.8	1.5	-0.3	0.6	24.3	16.9	2.4	1.0
			4σ	3.1	1.5	-0.3	0.7	28.7	20.2	2.9	1.3
			5σ	3.3	1.5	-0.3	0.8	39.1	41.6	3.4	1.9
			6σ	3.5	1.6	-0.3	1.0	45.5	45.5	4.1	2.9
		Median	25%	-0.2	1.1	-2.1	0.5	2.2	0.6	0.7	0.1
			37.5%	0.5	1.2	-1.4	0.5	3.1	1.1	0.7	0.2
			50%	1.3	1.5	-0.6	0.5	5.5	3.8	0.8	0.3
			62.5%	2.1	1.7	0.2	0.7	9.2	10.9	0.9	0.4
			75%	3.0	1.8	0.9	0.8	13.7	17.2	1.0	0.5
61519 CCD_S2 7/30/01	89	Mean	1σ	2.2	2.6	-0.1	0.7	11.9	6.0	1.4	0.5
			2σ	2.5	2.6	-0.0	0.8	16.9	11.2	1.8	0.7
			3σ	2.7	2.7	0.0	0.8	21.4	15.4	2.1	0.9
			4σ	2.9	2.7	-0.0	0.9	25.1	17.9	2.4	1.0
			5σ	3.1	2.7	-0.0	0.9	28.2	20.2	2.7	1.2
			6σ	3.2	2.7	0.0	1.0	33.9	31.6	3.0	1.6
		Median	25%	-0.0	1.9	-1.6	0.5	2.8	0.6	0.8	0.2
			37.5%	0.7	2.0	-0.9	0.6	3.8	0.9	0.8	0.2
			50%	1.5	2.8	-0.1	0.9	6.0	3.3	0.9	0.5
			62.5%	2.3	3.2	0.6	1.0	8.7	5.5	0.9	0.6
			75%	3.1	3.3	1.2	1.1	12.2	9.3	1.1	0.7
61507 CCD_I3 8/12/01	85	Mean	1σ	1.8	2.7	-0.9	0.6	13.7	15.0	1.5	0.5
			2σ	2.2	2.7	-0.8	0.7	18.9	19.7	2.0	0.8
			3σ	2.5	2.8	-0.7	0.8	23.5	23.3	2.4	1.2
			4σ	2.7	2.8	-0.7	1.0	36.8	55.4	3.1	2.7
			5σ	3.0	2.9	-0.7	1.2	43.3	63.1	3.8	4.1
			6σ	3.2	3.0	-0.7	1.4	48.5	65.9	4.4	4.6
		Median	25%	-0.5	1.7	-2.6	0.5	2.0	0.6	0.8	0.2
			37.5%	0.3	1.9	-1.9	0.5	3.0	0.9	0.8	0.2
			50%	1.1	3.1	-1.0	0.8	5.5	4.4	0.9	0.3
			62.5%	1.8	3.6	-0.3	0.7	7.8	6.4	0.9	0.3
			75%	2.7	3.7	0.4	0.6	17.5	36.3	1.2	1.1

a. The number of entire 512-row frames downlinked.
b. For the *Mean* algorithm, the rejection criterion; for the *Median* algorithm, the quartile taken.
c. After subtracting the mean overclock value.
d. Standard deviation over *n* runs of the value in the corresponding ADU column.

pair of typical frames is shown in Figure 2. The bias map that would result from this pair of frames is shown by the red points in Figure 3.

The frames of Figure 2 were chosen to best illustrate the effects of charge streaks parallel to the column direction. The strong streak of background charge in the bottom frame has caused the anomaly at column ~350 in

Figure 3, but the weaker streak on the right side of the bottom frame has had little effect on the bias map. In practice, we can expect some charge streaks to span across both frames, but we can t model this from the data since only the very first frames are contiguous, and these show systematic variations of background with row and output node that corrupt the analysis.

A second CC bias algorithm has been included with the ACIS flight software and may be selected by changing fields within the parameter blocks. This is the Median with *n*-quartile algorithm, and works as follows:[1]

1. After ignoring the first 100 frames, two consecutive frames (2×512 rows) are clocked from the CCD.
2. Each column is processed independently...
3. The 1024 pixels are sorted by value.
4. The m^{th} pixel in ascending order is chosen as the bias value for that column, where $m = 1024 * n / 100$.

The result of running this algorithm on the frames of Figure 2 is shown by the blue dots in Figure 3. The improvement is evident. Table 2 shows the result of applying the *Mean* and *Median* algorithms to successive pairs of n_f raw frames from the three runs, and varying the algorithm-dependent sub-parameters (*parm* = *n*σ-rejection and *n*% quartile, respectively).

Conclusions

1. Background charge in FI CCDs is responsible for the anomalously high bias map values. The best confirmation of this is the correlation within the limits of statistical uncertainty between the Δ_{mean}, Δ_{max}, and σ_Δ values in Table 1 and the corresponding values in Table 2 when the three raw-mode tests were processed by the on-orbit algorithm, *i.e.*, Mean with 5-σ rejection.
2. BI CCDs are unaffected.
3. The choice of Mean with 5-σ rejection for the on-orbit bias algorithm is far from optimal. In fact, the results from this algorithm applied to the raw-mode test data (outlined in red in Table 2) are almost maximally bad, relative both to the variance (σ_Δ) and peak (Δ_{max}) of the anomalous values!
4. The best currently available choice of bias algorithm appears to be the Median with 37.5% quartile (outlined in blue in Table 2). This can be selected by changing the following fields of all ACIS CC parameter blocks[2] from

```
biasAlgorithmId     =    0    0    0    0    0    0
biasRejection       =    5    5    5    5    5    5
```

   to

```
biasAlgorithmId     =    1    1    1    1    1    1
biasRejection       =  384  384  384  384  384  384
```

5. The advantages of changing the algorithm are in improved FI energy resolution and quantum efficiency (QE).
6. If this change is made, the mean bias value may be expected to decrease by 2 or 3 ADU (from a comparison of the Δ_{mean} values in Table 2). If it is thought desirable to achieve the same background suppression and hence the same false-event rates as the previous algorithm, FI event and split thresholds should be adjusted by changing

```
fep*EventThreshold  =   38   38   38   38   38   38
fep*SplitThreshold  =   13   13   13   13   13   13
```

to

```
fep*EventThreshold  =   41   41   41   41   41   41
fep*SplitThreshold  =   16   16   16   16   16   16
```

7. Bias map anomalies will have reduced the QE of FI CCDs in the existing 64 CC runs. We therefore expect that sources whose images lay on columns close to bias map anomalies would appear to vary in brightness as the observatory dithered the images through the bad bias columns and their events became indistinguishable from background noise. Recognizing this, it should be possible to reprocess these runs with suitably filtered bias maps, thereby determining the event energies to greater precision, although the loss of QE, and hence the correction to the exposure maps, will be difficult to estimate.
8. If subsequent observations use the *Median* algorithm, users must be warned that the average bias values will decrease by several ADU. This will affect the event energy calibration of CC runs, and also complicate the comparison of those runs against runs that use the existing *Mean* algorithm.
9. There is no particular reason to change the existing bias algorithm for BI CCDs, and no reason to suspect that BI bias maps are unreliable, so I recommend that we continue to use Mean with 5-σ rejection for them. The flight software is able to use different algorithms for each chip, and the ACIS uplink parameter block generation process, controlled by a Ruleset[3], is fully capable of assigning the algorithms appropriately.

References

1. ACIS Software Detailed Design Specification, MIT CSR 36-53200, Rev. 01, November 1995. (acis.mit.edu/acis/sdetail-01pp/sdetail.pdf) The CC bias algorithms are defined in ⁄45.6.
2. ACIS Instrument Parameters and Command Language, MIT CSR 36-53204.0204 Rev. N, March 2001. (acis.mit.edu/acis/ipcl) The CC parameters are defined in the *loadCcBlock* section.
3. ACIS Parameter Block Ruleset, MIT CSR Rev. 1.5, May 1999. (acis.mit.edu/axaf/napcat.html)